



Published in final edited form as:

Biochem Pharmacol. 2010 September 15; 80(6): 932–940. doi:10.1016/j.bcp.2010.05.007.

Ube2l3 gene expression is modulated by activation of the aryl hydrocarbon receptor: Implications for p53 ubiquitination

O.D. Reyes-Hernández^a, A. Mejía-García^b, E.M. Sánchez-Ocampo^b, M.A. Cabañas-Cortés^b, P. Ramírez^c, L. Chávez-González^d, F.J. Gonzalez^e, and G. Elizondo^{b,*}

^aDepartamento de Toxicología, CINVESTAV-IPN, Zacatenco. México D.F., Av. IPN 2508, C.P. 07360, Mexico

^bDepartamento de Biología Celular, CINVESTAV-IPN, Zacatenco. México D.F., Av. IPN 2508, C.P. 07360, Mexico

^cUnidad de Investigación Multidisciplinaria, Laboratorio de Toxicología y Genética, Facultad de Estudios Superiores Cuautitlán, UNAM, Cuautitlán Izcallí, Mexico

^dDNA Microarray Unit, UNAM, Mexico

^eLaboratory of Metabolism, NCI, National Institutes of Health, Bethesda, MD, United States

Abstract

Exposure to 2,3,7,8-tetrachlorodibenzo-p-dioxin (TCDD), a halogenated aromatic hydrocarbon and environmental contaminant, results in several deleterious effects, including fetal malformation and cancer. These effects are mediated by the aryl hydrocarbon receptor (AhR), a ligand-activated receptor that regulates the expression of genes encoding xenobiotic-metabolizing enzymes. Several reports suggest that AhR function is beyond the adaptive chemical response. In the present study, we analyzed and compared gene expression profiles of C57BL/6N wild-type (WT) and *Ahr*-null mice. DNA microarray and quantitative RT-PCR analyses revealed changes in the expression of genes involved in the ubiquitin-proteasome system (UPS). UPS has an important role in cellular homeostasis control and dysfunction of this pathway has been implicated in the development of several human pathologies. Protein ubiquitination is a multi-step enzymatic process that regulates the stability, function, and/or localization of the modified proteins. This system is highly regulated post-translationally by covalent modifications. However, little information regarding the transcriptional regulation of the genes encoding ubiquitin (Ub) proteins is available. Therefore, we investigated the role of the AhR in modulation of the UPS and regulation of Ube2l3 transcription, an E2 ubiquitin-conjugating enzyme, as well as the effects on p53 degradation. Our results indicate that AhR inactivation decreases on liver proteasome activity, probably due to a down-regulation on the expression of several proteasome subunits. On the other hand, AhR activation increases Ube2l3 mRNA and protein levels by controlling *Ube2l3* gene expression, resulting in increased p53 ubiquitination and degradation. In agreement with this, induction of apoptosis was attenuated by the AhR activation.

*Corresponding author. Tel.: +52 55 5747 3800x5555; fax: +52 55 5747 3393. gazuela@cinvestav.mx (G. Elizondo).

Keywords

AhR; Ubiquitin-proteasome system; Ube2l3; p53; TCDD

1. Introduction

Exposure to 2,3,7,8-tetrachlorodibenzo-p-dioxin (TCDD), a halogenated aromatic hydrocarbon, environmental contaminant, and the most toxic dioxin, results in several deleterious effects, including wasting syndrome, immunotoxicity, hepatotoxicity, fetal malformation, and cancer [1]. These effects are mediated by the aryl hydrocarbon receptor (AhR), a ligand-activated receptor that is a member of the basic helix-loop-helix/Per-Arnt-Sim (bHLH-PAS) transcription factor family. Upon binding TCDD, the AhR translocates to the nucleus, dimerizes with the AhR nuclear translocator protein (ARNT), binds xenobiotic responsive elements (XREs), and up-regulates the expression of a battery of genes encoding xenobiotic-metabolizing enzymes, such as the cytochrome P450s (CYP1A1, CYP1A2, CYP1B1), NAD(P)H quinone oxydoreductase, and UDP-glucuronosyl-transferase 6 [2]. Although AhR may function as part of an adaptive chemical response, several studies suggest that this transcription factor could have important functions in liver and cardiac development [3,4], cell proliferation [5], homeostasis of the immune system [6], circadian rhythmicity, and cholesterol and glucose metabolism [7,8].

In order to understand the physiologic role of AhR and identify genes under its control, we compared the basal liver gene expression between *Ahr*-null and wild-type (WT) mice by DNA microarray analysis. Results suggested that AhR may control the expression of hundred of genes that participate in various cell processes, such as metabolism, glycolysis, and gluconeogenesis. Of interest, microarray analysis also indicates that expression of several genes encoding for ubiquitin-proteasome system (UPS) proteins was altered. The UPS is a specific, non-lysosomal pathway responsible for the degradation of short-lived and abnormal/mutated intracellular proteins involved in several cell processes, such as cell cycle progression, development, cell death, and elimination of abnormal proteins by mutation and oxidation [9–11]. The dysfunction of this system is associated with the development of human pathologies such as tumorigenesis, neurodegenerative diseases, and immune system disorders.

Ubiquitination is a multiple enzyme process that begins when ubiquitin-activating enzyme, or E1, recruits ubiquitin (Ub) in an ATP-dependent manner. E1 then transfers Ub to the ubiquitin-conjugating enzyme, or E2. The ubiquitin-E2 complex binds to the ubiquitin-protein ligase, or E3, which recognizes the target protein and facilitates the transfer of Ub from E2 to the substrate. Finally, the ubiquitylated target protein is usually recognized and degraded by the 26S proteasome. This system is highly regulated post-translationally by covalent modification such as phosphorylation or ubiquitination [12]. However, little information regarding the transcriptional regulation of the genes encoding Ub proteins is available. Among the genes encoding for UPS proteins, the present microarray analysis suggests that gene expression of Ube2l3, an E2 Ub protein, may be under AhR control. Ube2l3, also known as UbcH7, L-UBC, UbcM4, or E2-F1, is an 18-kDa protein involved in

the regulation of several cell processes, such as cell proliferation [13], and regulation of p53 [14], c-fos [15], and nuclear receptors such as glucocorticoid [16] and progesterone receptors [17]. The goal of the present study was to determine whether Ahr is involved in the modulation of the UPS, as well as to evaluate the role of the AhR in Ube2l3 transcriptional regulation and the p53 degradation.

2. Materials and methods

2.1. Materials

TCDD was purchased from AccuStandard (New Haven, CT). Triton X-100, benzo[*a*]pyrene (B[*a*]P), and griseofulvin were purchased from Sigma (St. Louis, MO). N-ethylmaleimide was acquired from Pierce (Rockford, IL).

2.2. Animals

The development of *Ahr*-null mice has been described previously [3]. Genotypes were determined by PCR as reported elsewhere [6]. WT littermates were used as control mice. Animals were randomly distributed ($n = 5$) and housed in a pathogen-free facility and fed with autoclaved Purina rodent chow (St. Louis, MO) with water available *ad libitum*. All animal studies were performed according to the Guide for the Care and Use of Laboratory Animals, as adopted and enforced by the U.S. National Institutes of Health, and the Mexican Regulation of Animal Care and Maintenance (NOM-062-ZOO-1999, 2001).

2.3. Treatments

TCDD was diluted in corn oil at a concentration such that the intended dose would be delivered in 100 μ l. Each male mouse, aged 6–8 weeks, was given single or repeated intraperitoneal (i.p.) doses of 80 μ g TCDD/kg body weight, or an equivalent volume of corn oil (control). B[*a*]P, diluted in corn oil, was given i.p. at 230 mg/kg body weight. Animals were treated by gavage with a single dose (5 mg/kg body weight) griseofulvin, diluted in corn oil, for 9 days. After treatments, mice were euthanized by cervical dislocation, and livers were removed, frozen in liquid nitrogen, and stored at -70 °C.

2.4. Microarray assay

In each group, equivalent amounts of RNA from individual animals were pooled and used for cDNA synthesis, incorporating dUTP-Cy3 or dUTP-Cy5 using the CyScribe First-Strand cDNA labeling kit (Amersham, Sunnyvale, CA). Following labeling and purification, Cy3- and Cy5-labeled cDNA were hybridized to 22 000 gene-specific oligonucleotide probes representing 70% of the mouse genome. For array printing, a Mouse 65-mer oligo library from the Sigma-Genosys oligo sets was used. The data acquisition and quantification of array images was performed in a ScanArray 4000 microarray analysis system using the accompanying software (Packard BioScience, CT). All images were captured using 65% PMT gain, 70–75% laser power and 10 μ m resolution at 50% scan rate. For each spot, the Cy3 and Cy5 density mean value and the Cy3 and Cy5 background mean value were calculated with ArrayPro Analyzer software (Media Cybernetics).

Microarray data analysis was performed using the free software genArise, developed in the Computing Unit of the Cellular Physiology Institute of Autonomous National University of Mexico (<http://www.ifc.unam.mx/genarise/>, 2009). GenArise performs a number of transformations: background correction, lowest normalization, intensity filter, replicates analysis and selecting differentially expressed genes. The software identifies differential expressed genes by calculating an intensity-dependent z -score. Using a sliding window algorithm to calculate the mean and the standard deviation within a window surrounding each data point, the software determines the z -score, where z measures the number of standard deviations a data point is from the mean: $z_i = [R_i - \text{mean}(R)]/\text{sd}(R)$; where z_i is the z -score for each element, R_i is the log-ratio for each element, and $\text{sd}(R)$ is the standard deviation of the log-ratio. With this criterion, the elements with a z -score greater than 2 standard deviations were identified as differentially expressed genes.

2.5. Proteasome assays

Proteasome activity was determined using Suc-LY-AMC (Boston Biochem, Cambridge, MA) as a proteasome-specific substrate. Liver homogenates were prepared in buffer A (50 mM Tris-HCl, pH 7.5; 150 mM NaCl; 0.5 mM EDTA; 0.5% Nonidet P40). Chymotrypsin-like activity of the 20S proteasome was assayed by adding 50 μg protein to 1 ml buffer A containing 10 μM fluorescent substrate. After incubation at 37 °C for 30 min, the reaction was stopped at 4 °C. Fluorescence was measured using a VersaFluor Fluorometer (Bio-Rad, Hercules, CA) with excitation and emission wavelengths of 360 and 480 nm, respectively. Background fluorescence was determined from negative control reactions.

2.6. Western blot analysis

Liver fragments were homogenized in buffer containing 10 mM Tris-HCl pH 7.4, 1% Nonidet P40, 10 $\mu\text{g}/\text{ml}$ aprotinin, 10 $\mu\text{g}/\text{ml}$ leupeptin, 10 $\mu\text{g}/\text{ml}$ soybean trypsin inhibitor, and 1 mM PMSF. When detecting Ub, 10 mM N-ethylmaleimide was added to prevent deubiquitination [18]. Protein concentrations were determined using the Bradford reaction (Bio-Rad). Aliquots (20 μg) were solubilized in sample buffer [60 mM Tris-HCl, pH 6.8; 2% sodium dodecylsulfate (SDS); 20% glycerol; 2% mercaptoethanol; 0.001% bromophenol blue] and subjected to 12% SDS-polyacrylamide gel electrophoresis. Protein extracts were transferred to a nitrocellulose membrane using a mini trans-blot (Bio-Rad). The transfer was performed at a constant voltage of 80 V for 2 h in a transfer buffer (48 mM Tris-HCl, 39 mM glycine, pH 8.3; 20% methanol). Following the transfer, membranes were blocked overnight at 4 °C in the presence of 2% nonfat dry milk and 0.5% bovine serum albumin (BSA) in blocking buffer (25 mM Tris-HCl, pH 7.5; 150 mM NaCl) and subsequently incubated at 4 °C for 3 h with goat polyclonal anti-Ube2l3 (1:5000; Abcam, Cambridge, MA), mouse anti-Ub (1:100; Zymed, San Francisco, CA), or actin (1:1000; Zymed) diluted in buffer (25 mM Tris-HCl, pH 7.5; 150 mM NaCl; 0.1% Tween 20; 0.05% nonfat dry milk; 0.05% BSA). After washing, the membranes were incubated with corresponding horseradish peroxidase (HRP)-conjugated secondary antibodies: HRP-goat anti-mouse IgG (Zymed), or HRP-rabbit anti-goat IgG (Pierce), for 2 h at 4 °C. The membrane was washed, and the immunoreactive protein was detected using an ECL Western blotting detection kit (Amersham, Arlington Heights, IL). The integrated optical density of the bands was quantified using scanning densitometry (GS-800 Calibrated Densitometer, Bio-Rad).

2.7. Real-time quantitative PCR (RT-PCR) analysis

Briefly, total RNA was prepared from mouse liver using the TRIzol reagent according to the manufacturer's instructions (Invitrogen, Camarillo, CA). RNA was quantified spectrophotometrically at OD₂₆₀. Subsequently, RNA integrity was evaluated by electrophoresis of RNA samples on 1% agarose gels. cDNA for the quantitative PCR assay was prepared from 2 µg total RNA using the SuperScript First-Strand Synthesis (Invitrogen), and oligo dT. PCR reactions were conducted using an ABI PRISM 7000 Sequence Detector System (Applied Biosystems, Branchburg, NJ) and analyzed using the comparative threshold cycle (Ct) method, as described previously [19]. The genes encoding Ube213 or 18S ribosomal RNA (rRNA, endogenous) were amplified in a single PCR reaction to allow for normalization of the mRNA data. The PCR reaction mixture contained 2 µl of cDNA, 1xTaqMan Universal PCR Master Mix (Applied Biosystems) and 0.9 and 0.25 µM primers and probes, respectively. The primers and probes sequences used for Ube213 were: 5'-TGCCAGTCATTAGTGCTGAAAAC-3' (forward), 5'-GGGTCATTCACCAGTGCTATGAG-3' (reverse), and probe (FAM): AAGACTGACCAAGTAATCC.

2.8. In silico analysis

The mouse *Ube213* gene promoter was analyzed using the follow web-based bioinformatic tools: Genomatix (http://www.genomatix.de/cgi-bin/matinspector_prof/mat_fam.pl?s=eabd9a3f188f5b276aaa00a3445cdcbe, 2009) and CBRC (<http://www.cbrc.jp/research/db/TFSEARCH.html>, 2009).

2.9. Chromatin immunoprecipitation

The ChiP assay was performed according to the kit protocol (Santa Cruz Biotechnology, Visalia, CA) using an AhR antibody (Thermo Scientific, Suwanee, GA). The PCR product corresponding to the *Ube213* proximal promoter was generated from an aliquot of the immunoprecipitated material. Briefly, hepatocytes from WT mice were washed with PBS buffer, and cross-linking induced with formaldehyde (1%). After chromatin isolation, the DNA was fragmented, and immunoprecipitation was performed. The cross-linking was reversed, the DNA was purified, and PCR amplification was performed as follows: initial denaturation (94 °C, 2 min), 35 cycles of denaturation (94 °C, 30 s), annealing (67 °C, 30 s), and extension (72 °C, 3 min). A final extension cycle (72 °C, 10 min) was added. Forward and reverse primers were as follows: 5'-CCCCCCTGGGGTACCAAAGAAGTAGTAGGCCTGAAGAGATTG-3' (forward) and 5'-CTGAAGCTTTCCCAAATGCATCGCGGTAGGCCAGGC-3' (reverse).

2.10. Immunoprecipitation

Liver protein extracts (20 µg) were adjusted to 300 µl with lysis buffer (plus 10 mM N-ethylmaleimide to prevent deubiquitination), and, after addition of the primary antibody, mouse anti-p53 (Zymed), samples were incubated overnight at 4 °C. The next day, 10 µl protein A sepharose was added and incubated, with shaking, for 1 h at 4 °C. After centrifugation (13 000 rpm), the pellet was washed once with TNET buffer (150 mM NaCl, 50 mM Tris, pH 7.5; 5 mM EDTA; 1% Triton X-100), twice with TNE buffer (150 mM

NaCl, 50 mM Tris, pH 7.5; 5 mM EDTA), and once with H₂O. Finally, pellet was resuspended in 10 µl 2X SDS sample loading buffer. Ub coupled to p53 were detected using same protocol, with an anti-Ub antibody as the primary.

2.11. Detecting apoptosis

WT and *Ahr*-null mice were treated with B[a]P, or pre-treated with TCDD and then exposed to B[a]P. Animals were anesthetized, bled and euthanized by cervical dislocation. The livers were paraffin-embedded and stained with hematoxylin and eosin (H&E) and examined by phase contrast microscopy. Apoptotic cells were detected using the DeadEnd Td T-mediated X-dUTP nick end labeling (TUNEL) System Kit according to the included protocol (Promega, Madison, WI).

2.12. Statistical analysis

Results are presented as the mean values \pm the standard deviation (S.D.) or the standard error (S.E.). The statistical significance of the data was evaluated using Mann-Whitney's U-Wilcoxon rank or the Student's *t*-test, as appropriate. In all cases, the differences between animal groups were considered to be statistically significant when the *P* value was less than 0.05.

3. Results

To investigate the role of the AhR on basal gene expression, we compared liver gene expression patterns of WT and *Ahr*-null mice by DNA microarray analysis. Transcripts with expression changes of 1.5 times or more, relative to WT, were selected. AhR disruption affected 2190 transcripts; of these, 1280 were down-regulated and 910 were up-regulated. Table 1 shows a list of genes, involved in several cell processes, whose expression was down-regulated in *Ahr*-null liver mouse. Some of these genes have been reported previously, such as those involved in xenobiotic responses. However, the present microarray analysis indicated that others genes unrelated to direct xenobiotic response may be under AhR regulation. Among these are genes encoding proteins belonging to the UPS. In order to confirm an alteration in the UPS, we first determined proteasome activity. Liver tissue from *Ahr*-null mice had decreased proteasome activity compared with WT mice (Fig. 1). We then examined whether TCDD modifies the chymotrypsin-like activity of the 20S proteasome. TCDD treatment decreased the proteasome activity in both WT and *Ahr*-null mice. The magnitude of the TCDD effect was similar to that induced by griseofulvin, a proteasome inhibitor. Western blot analysis was performed to determine whether decreased proteasome activity modifies the level of ubiquitin-conjugated proteins. *Ahr*-null mice had higher levels of ubiquitin-conjugated proteins compared to WT mice (Fig. 2A). These results are in agreement with the low proteasome activity observed in the AhR-null mice. As expected, TCDD treatment induced an increase in ubiquitin-conjugated proteins, which was more marked in wild-type than *Ahr*-null mouse when compared to their respective controls (Fig. 2B and C).

Among the genes with altered expression, Ube2l3 had the highest *z*-score (Table 1). In agreement with the microarray analysis, quantitative RT-PCR revealed that Ube2l3 mRNA

levels decreased 4-fold in *Ahr*-null mice compared to WT mice. Moreover, TCDD treatment resulted in a 4-fold induction of *Ube2l3* mRNA levels compared to the control group (Fig. 3A). We then investigated whether the increase in *Ube2l3* mRNA levels induced by TCDD reflects changes in *Ube2l3* protein levels. Indeed, Western blot analysis indicated that TCDD treatment induced a 2-fold increase in *Ube2l3* protein levels after 48 and 72 h (Fig. 3B). These data suggest that both basal gene expression and induction *Ube2l3* are under AhR control.

In order to identify putative xenobiotic response elements (XREs) in the mouse *Ube2l3* gene promoter, we performed *in silico* analysis. Common regulatory sequences, such as the TATA box, HNF-3b, GATA, p300, and AP1, were located between position -674 and the putative transcription start site. More importantly, two putative XREs were identified at positions -581 and -3520 (Fig. 4A). To determine whether AhR binds to the *Ube2l3* gene promoter, a ChIP assay was performed. WT mice were treated with TCDD or vehicle, and cell extracts from the liver were obtained. Chromatin was immunoprecipitated with the AhR antibody, and DNA from the precipitates was used for PCR analysis, using a primer pair that includes the putative XRE located at -581. AhR was associated with this regulatory region. Moreover, AhR activation by TCDD increased this interaction (Fig. 4B). The above results suggest that *Ube2l3* gene induction is mediated by AhR through its interaction with the -2252/+18 region, probably to the XRE located at -581.

We then explored whether AhR activation increase ubiquitination and degradation of p53, an *Ube2l3* substrate. After TCDD treatment, WT mice had decreased p53 protein levels, an effect that was not observed in *Ahr*-null mice (Fig. 5A). Immunoprecipitation studies were performed to determine whether this p53 decrease is associated with an increase in p53 ubiquitination. AhR activation by TCDD increased levels of ubiquitylated p53 (Fig. 5B). To examine the implications of p53 ubiquitination, apoptosis in hepatocytes from WT and *Ahr*-null mouse was evaluated by the TUNEL assay and morphology of H&E stained cells. *Ahr*-null control hepatocytes had a 2-fold increase in the number of apoptotic cells compared to WT control cells (Fig. 7). As shown in Figs. 6 and 7, WT mice had a 10-fold increase in apoptotic cells after B[a]P treatment. This effect was attenuated by TCDD pre-treatment. As expected, *Ahr*-null mouse were resistant to the toxic effects of B[a]P treatment.

4. Discussion

The UPS targets proteins for degradation and has a critical role in multiple cellular processes, including differentiation, cell cycle regulation, transport, embryogenesis, immune responses, apoptosis, and control of signal transduction [20–23]. Therefore, it is not surprising that alterations in this system result in the development of several pathologies, such as malignancies, neurologic diseases, and immune system disorders [24,25]. The Ub proteins are tightly regulated, mainly at the post-translational level, by phosphorylation or ubiquitination. However, little information regarding the transcriptional regulation of the genes encoding Ub proteins is available.

The evidence of the AhR participation in the UPS was suggested by studies showing that ER α proteasome-dependent degradation was promoted by the AhR [26]. More recently, it

has been shown that the AhR acts as a ligand-dependent E3 ubiquitin ligase promoting the proteolysis of estrogen and androgen receptors [27,28], as well as β -catenin [29]. In the present study, the data suggest that the AhR, a ligand-dependent transcription factor, has a role in the regulation of the UPS by controlling the expression levels of certain proteins. A decrease in proteasome activity in the liver of *Ahr*-null mice compared to WT mouse was observed, together with an increase in total ubiquitylated-protein levels. These results may be explained by decreased expression of the Psm12, Psm2 and Psm3 proteasome subunits (Table 1). Psm12, also named Rpn5, is a subunit of the 19S proteasome, and constitutes part of the lid structure while Psm2 and Psm3, also known as the β 4 and β 2 subunits, respectively, are part of the 20S core particle, which is responsible for proteolysis. Therefore, decrease expression of these proteasome subunits may result in an impaired ubiquitinated protein recognition, as well as compromised proteolytic function of the proteasome. Although in the present study the Psm12, Psm2 and Psm3 expression data from the microarray analysis were not validated, other proteomic and genomic approaches suggest that the expression of several proteasome subunits is under AhR control. In a recent study, Tijet et al. [30] mapped the AhR-dependent genes. Among them, proteasome activator subunit 4 and proteasome subunit β 5 showed an AhR-dependent expression. Moreover, salmon hepatocytes treated with TCB (3,3',4,4'-tetrachlorobiphenyl), an AhR agonist, had increased proteasome β subunit mRNA levels. This effect is blocked by the AhR antagonist α -naphtho-flavone [31]. On the other hand, proteome analysis in Jurkat cells showed that proteasome β 7 subunit protein level increased significantly after benzo[*a*]pyrene treatment [32]. Furthermore, rats treated with TCDD also have increased proteasome subunit β 3 protein levels [33].

When animals were treated with TCDD, inhibition of proteasome activity, in both WT and *Ahr*-null mice was observed, which was similar to that induced by griseofulvin. These last results suggest that the proteasome inhibitory effects of TCDD are AhR-independent, and may be the result of general toxicity rather than a specific action. As expected, inhibition of proteasome activity by TCDD also results in an accumulation of ubiquitylated proteins, although this effect was more marked in *Ahr*-null mice.

Because Ube213, an E2 enzyme, is involved in the ubiquitin-dependent proteolysis of important molecules such as p53, we decided to determine whether this protein expression is under AhR control. Quantitative RT-PCR revealed that Ube213 mRNA level is 4-fold decreased in the liver of *Ahr*-null mice compared to WT mice. Conversely, when AhR was activated by TCDD treatment a 4-fold induction was observed in WT but not in *Ahr*-null mouse. These results suggested that both basal gene expression and induction of *Ube213* are AhR-dependent, which was confirmed by *in silico* and ChIP analysis. The *Ube213* gene promoter has two putative XREs; AhR interact with a promoter region that includes the -581 XRE, and this interaction is stimulated by TCDD. AhR-TCDD dependent up-regulation of Ube213 mRNA increases Ube213 protein expression in a time-dependent manner. To our knowledge, this is the first report establishing a mechanism of *Ube213* gene expression control, which suggests the potential use of AhR as a therapeutic target in order to modulate the degradation of Ube213 substrates such as p53.

The p53 gene is mutated in approximately 50% of human cancers [34] even though it is tightly regulated at several levels. Among these, post-translational modification, including ubiquitination, has an important role in p53 regulation and therefore in tumorigenesis. The evidence that p53 is modified by the UPS arose from studies that determined that p53 degradation was increased in cells expressing the E6/HPV oncogenic protein. This led to the discovery that E6 activated and redirected E6AP [35], an E3 Ub ligase, to promoting p53 degradation. E6AP also interacts with Ube2l3, and this complex participates in p53 ubiquitination [36]. Accordingly, the present results show that TCDD treatment, most likely by inducing Ube2l3 expression, increases Ub-p53 while decreasing overall p53 protein levels. Moreover, TCDD pre-treatment attenuated B[a]P-induced apoptosis in WT mice. These data support the idea that AhR activation might promote p53 degradation and, therefore, inhibit apoptosis. In agreement with these results, Paajarvi et al. [37] reported that TCDD decreases the p53 response to DNA damage, and suggested that this effect is AhR-dependent through an increase in Mdm2, an E3 Ub ligase and the primary regulator of p53. However, TCDD only increased Mdm2 protein levels, but not Mdm2 mRNA. In addition, the UV-induced p53 response was attenuated by TCDD [38]. These studies, together with the present data, support the hypothesis that the AhR regulates the UPS by controlling the expression of Ub proteins as well as certain proteasome catalytic subunits. In particular, the present study indicates that AhR might regulate p53 degradation by controlling *Ube2l3* gene expression (Fig. 8). Therefore, high Ube2l3 and Mdm2 levels would decrease the p53 response to DNA damage and might contribute to individual susceptibility to cancer.

On the other hand, untreated *Ahr*-null livers exhibit higher levels of apoptotic cells compared to WT samples. However, p53 basal levels are similar between both, wild-type and *Ahr*-null mice. This same phenotype was observed in cultures of mouse embryonic fibroblast (MEFs) and hepatocytes from *Ahr*-null mice where high levels of apoptosis in association with a cell cycle arrest were observed. Hepatocytes and MEFs from *Ahr*-null mouse also presented high levels of *TGFb* [5,39]. Therefore, the increased apoptosis level may be explained by the increased levels of this cytokine.

Collectively, the present data suggest that the AhR may be part of a new signaling mechanism through which UPS-dependent degradation is modulated. As such, further research is needed in order to better understand the molecular mechanisms by which the AhR controls ubiquitin-proteasome system gene expression. These results also identify the AhR as an interesting pharmacological target to treat certain cancers and neurological diseases that result from dysregulation of p53 levels. The development of AhR agonists and antagonists with non-toxic effects would be a crucial first step.

Acknowledgments

We thank Simón Guzmán León, José Luis Santillán Torres and Jorge Ramírez for technical assistance with the microarrays, and Gerardo Coello, Gustavo Corral and Ana Patricia Gómez for assistance with the genArise software. We also thank Samia Fattel Fazenda for technical assistance with the TUNEL assay. This work was supported by CONACYT grant 48786.

References

- [1]. Huff J, Lucier G, Tritscher A. Carcinogenicity of TCDD: experimental, mechanistic, and epidemiologic evidence. *Annu Rev Pharmacol Toxicol* 1994;34:343–72. [PubMed: 8042855]
- [2]. Gonzalez FJ, Fernandez-Salguero P. The aryl hydrocarbon receptor: studies using the AHR-null mice. *Drug Metab Dispos* 1998;26(12):1194–8. [PubMed: 9860927]
- [3]. Fernandez-Salguero P, Pineau T, Hilbert DM, McPhail T, Lee SS, Kimura S, et al. Immune system impairment and hepatic fibrosis in mice lacking the dioxin-binding Ah receptor. *Science* 1995;268(5211):722–6. [PubMed: 7732381]
- [4]. Fernandez-Salguero PM, Ward JM, Sundberg JP, Gonzalez FJ. Lesions of aryl-hydrocarbon receptor-deficient mice. *Vet Pathol* 1997;34(6):605–14. [PubMed: 9396142]
- [5]. Elizondo G, Fernandez-Salguero P, Sheikh MS, Kim GY, Fornace AJ, Lee KS, et al. Altered cell cycle control at the G(2)/M phases in aryl hydrocarbon receptor-null embryo fibroblast. *Mol Pharmacol* 2000;57(5):1056–63. [PubMed: 10779392]
- [6]. Rodriguez-Sosa M, Elizondo G, Lopez-Duran RM, Rivera I, Gonzalez FJ, Vega L. Overproduction of IFN-gamma and IL-12 in AhR-null mice. *FEBS Lett* 2005;579(28):6403–10. [PubMed: 16289099]
- [7]. Sato S, Shirakawa H, Tomita S, Ohsaki Y, Haketa K, Tooi O, et al. Low-dose dioxins alter gene expression related to cholesterol biosynthesis, lipogenesis, and glucose metabolism through the aryl hydrocarbon receptor-mediated pathway in mouse liver. *Toxicol Appl Pharmacol* 2008;229(1):10–9. [PubMed: 18295293]
- [8]. Reyes-Hernandez OD, Mejia-Garcia A, Sanchez-Ocampo EM, Castro-Muno-zledo F, Hernandez-Munoz R, Elizondo G. Aromatic hydrocarbons upregulate glyceraldehyde-3-phosphate dehydrogenase and induce changes in actin cytoskeleton. Role of the aryl hydrocarbon receptor (AhR). *Toxicology* 2009;266(1–3):30–7. [PubMed: 19850099]
- [9]. Demasi M, Davies KJ. Proteasome inhibitors induce intracellular protein aggregation and cell death by an oxygen-dependent mechanism. *FEBS Lett* 2003;542(1–3):89–94. [PubMed: 12729904]
- [10]. Sitte N, Merker K, Von Zglinicki T, Davies KJ, Grune T. Protein oxidation and degradation during cellular senescence of human BJ fibroblasts: Part II. Aging of nondividing cells. *FASEB J* 2000;14(15):2503–10. [PubMed: 11099468]
- [11]. Grune T, Reinheckel T, Davies KJ. Degradation of oxidized proteins in mam-malian cells. *FASEB J* 1997;11(7):526–34. [PubMed: 9212076]
- [12]. Deshaies RJ, Joazeiro CA. RING domain E3 ubiquitin ligases. *Annu Rev Biochem* 2009;78:399–434. [PubMed: 19489725]
- [13]. Whitcomb EA, Dudek EJ, Liu Q, Taylor A. Novel control of S phase of the cell cycle by ubiquitin-conjugating enzyme H7. *Mol Biol Cell* 2009;20(1):1–9. [PubMed: 18946090]
- [14]. Scheffner M, Huibregtse JM, Vierstra RD, Howley PM. The HPV-16 E6 and E6-AP complex functions as a ubiquitin-protein ligase in the ubiquitination of p53. *Cell* 1993;75(3):495–505. [PubMed: 8221889]
- [15]. Stancovski I, Gonen H, Orian A, Schwartz AL, Ciechanover A. Degradation of the proto-oncogene product c-Fos by the ubiquitin proteolytic system in vivo and in vitro: identification and characterization of the conjugating enzymes. *Mol Cell Biol* 1995;15(12):7106–16. [PubMed: 8524278]
- [16]. Garside H, Waters C, Berry A, Rice L, Ardley HC, White A, et al. Ubch7 interacts with the glucocorticoid receptor and mediates receptor autoregulation. *J Endocrinol* 2006;190(3):621–9. [PubMed: 17003263]
- [17]. Verma S, Ismail A, Gao X, Fu G, Li X, O'Malley BW, et al. The ubiquitin-conjugating enzyme UBCH7 acts as a coactivator for steroid hormone receptors. *Mol Cell Biol* 2004;24(19):8716–26. [PubMed: 15367689]
- [18]. Mimnaugh EG, Neckers LM. Measuring ubiquitin conjugation in cells. *Methods Mol Biol* 2005;301:223–41. [PubMed: 15917635]
- [19]. Medina-Diaz IM, Elizondo G. Transcriptional induction of CYP3A4 by o,p'-DDT in HepG2 cells. *Toxicol Lett* 2005;157(1):41–7. [PubMed: 15795092]

- [20]. DeMartino GN, Slaughter CA. The proteasome, a novel protease regulated by multiple mechanisms. *J Biol Chem* 1999;274(32):22123–6. [PubMed: 10428771]
- [21]. Freemont PS. RING for destruction? *Curr Biol* 2000;10(2):R84–7. [PubMed: 10662664]
- [22]. Kornitzer D, Ciechanover A. Modes of regulation of ubiquitin-mediated protein degradation. *J Cell Physiol* 2000;182(1):1–11. [PubMed: 10567911]
- [23]. Pickart CM. Mechanisms underlying ubiquitination. *Annu Rev Biochem* 2001;70:503–33. [PubMed: 11395416]
- [24]. Ciechanover A The ubiquitin proteolytic system and pathogenesis of human diseases: a novel platform for mechanism-based drug targeting. *Biochem Soc Trans* 2003;31(2):474–81. [PubMed: 12653666]
- [25]. Ciechanover A, Iwai K. The ubiquitin system: from basic mechanisms to the patient bed. *IUBMB Life* 2004;56(4):193–201. [PubMed: 15230346]
- [26]. Wormke M, Stoner M, Saville B, Safe S. Crosstalk between estrogen receptor alpha and the aryl hydrocarbon receptor in breast cancer cells involves unidirectional activation of proteasomes. *FEBS Lett* 2000;478(1–2):109–12. [PubMed: 10922479]
- [27]. Ohtake F, Baba A, Takada I, Okada M, Iwasaki K, Miki H, et al. Dioxin receptor is a ligand-dependent E3 ubiquitin ligase. *Nature* 2007;446(7135):562–6. [PubMed: 17392787]
- [28]. Ohtake F, Fujii-Kuriyama Y, Kato S. AhR acts as an E3 ubiquitin ligase to modulate steroid receptor functions. *Biochem Pharmacol* 2009;77(4):474–84. [PubMed: 18838062]
- [29]. Kawajiri K, Kobayashi Y, Ohtake F, Ikuta T, Matsushima Y, Mimura J, et al. Aryl hydrocarbon receptor suppresses intestinal carcinogenesis in ApcMin/+ mice with natural ligands. *Proc Natl Acad Sci U S A* 2009;106(32):13481–6. [PubMed: 19651607]
- [30]. Tijet N, Boutros PC, Moffat ID, Okey AB, Tuomisto J, Pohjanvirta R. Aryl hydrocarbon receptor regulates distinct dioxin-dependent and dioxin-independent gene batteries. *Mol Pharmacol* 2006;69(1):140–53. [PubMed: 16214954]
- [31]. Mortensen AS, Arukwe A. Targeted salmon gene array (SalArray): a toxico-genomic tool for gene expression profiling of interactions between estrogen and aryl hydrocarbon receptor signalling pathways. *Chem Res Toxicol* 2007;20(3):474–88. [PubMed: 17291011]
- [32]. Oh S, Im H, Oh E, Lee J, Khim JY, Mun J, et al. Effects of benzo(a)pyrene on protein expression in Jurkat T-cells. *Proteomics* 2004;4(11):3514–26. [PubMed: 15529408]
- [33]. Lee SH, Lee DY, Son WK, Joo WA, Kim CW. Proteomic characterization of rat liver exposed to 2,3,7,8-tetrachlorobenzo-p-dioxin. *J Proteome Res* 2005;4(2): 335–43. [PubMed: 15822908]
- [34]. Soussi T, Beroud C. Assessing TP53 status in human tumours to evaluate clinical outcome. *Nat Rev Cancer* 2001;1(3):233–40. [PubMed: 11902578]
- [35]. Huibregtse JM, Scheffner M, Howley PM. A cellular protein mediates association of p53 with the E6 oncoprotein of human papillomavirus types 16 or 18. *EMBO J* 1991;10(13):4129–35. [PubMed: 1661671]
- [36]. Ciechanover A, Shkedy D, Oren M, Bercovich B. Degradation of the tumor suppressor protein p53 by the ubiquitin-mediated proteolytic system requires a novel species of ubiquitin-carrier protein, E2. *J Biol Chem* 1994;269(13): 9582–9. [PubMed: 8144545]
- [37]. Paajarvi G, Viluksela M, Pohjanvirta R, Stenius U, Hogberg J. TCDD activates Mdm2 and attenuates the p53 response to DNA damaging agents. *Carcino-genesis* 2005;26(1):201–8.
- [38]. Worner W, Schrenk D. Influence of liver tumor promoters on apoptosis in rat hepatocytes induced by 2-acetylaminofluorene, ultraviolet light, or transforming growth factor beta 1. *Cancer Res* 1996;56(6):1272–8. [PubMed: 8640813]
- [39]. Zaher H, Fernandez-Salguero PM, Letterio J, Sheikh MS, Fornace AJ Jr, Roberts AB, et al. The involvement of aryl hydrocarbon receptor in the activation of transforming growth factor-beta and apoptosis. *Mol Pharmacol* 1998;54(2): 313–21. [PubMed: 9687573]

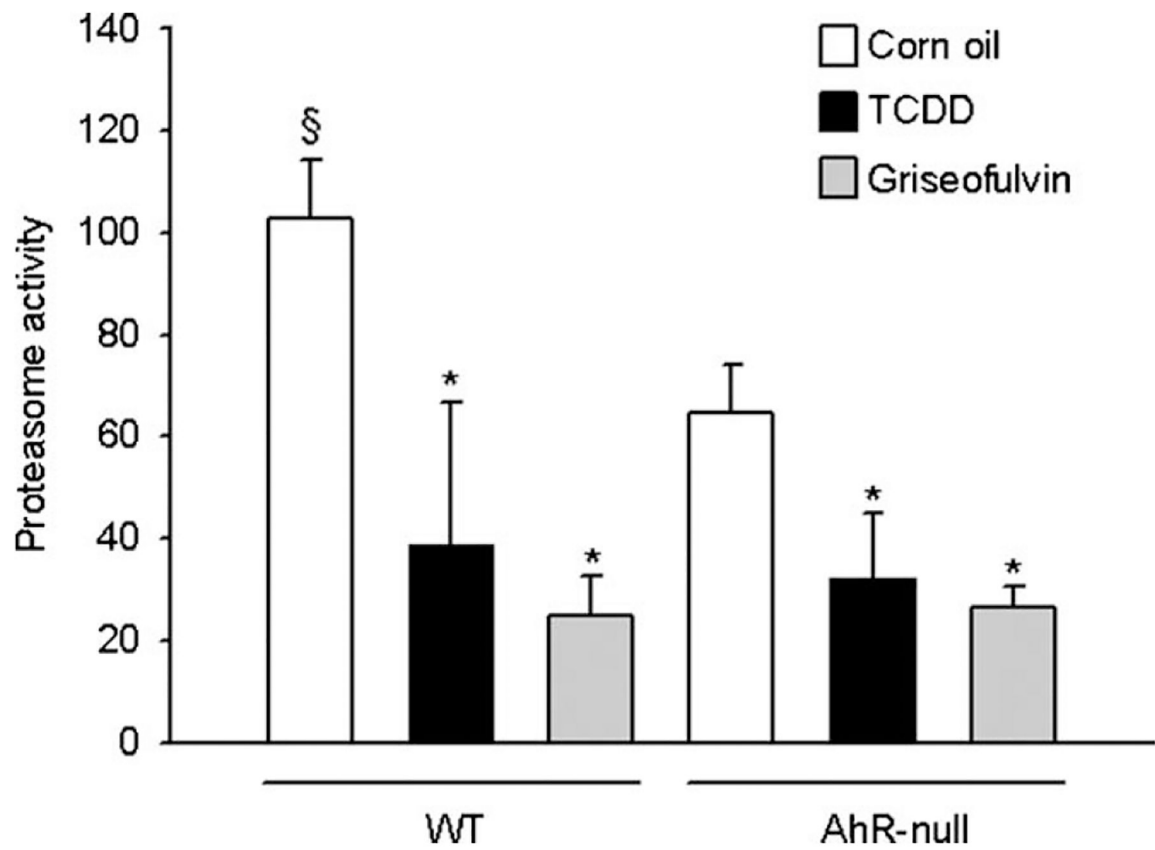


Fig. 1. *Ahr*-null mice have decreased proteasome activity. Mice were treated with 80 μ g TCDD/kg, 5 mg/kg griseofulvin, or vehicle. Liver samples were removed, and chymotrypsin-like activity of the 20S proteasome was determined as described in Section 2. Data represent mean values \pm S.D. * P < 0.05 vs. control (vehicle), § P < 0.05 vs. *Ahr*-null control.

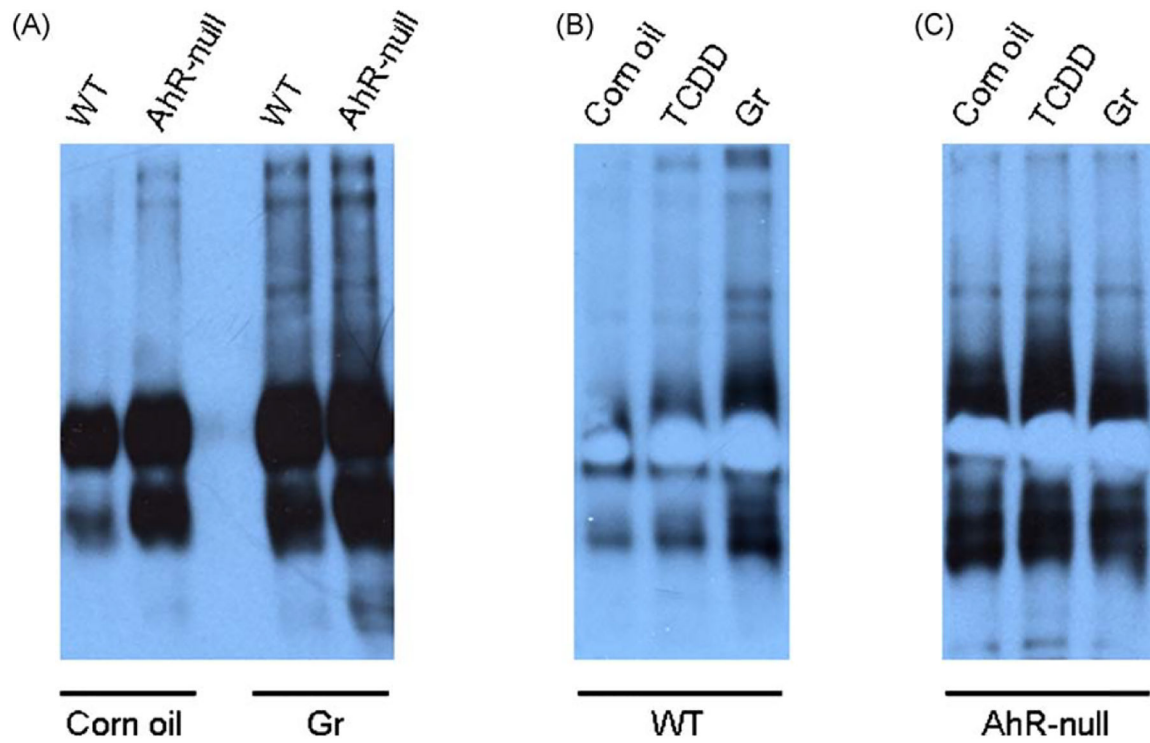


Fig. 2. Accumulation of Ub-conjugated proteins in *Ahr*-null mice. Basal levels of Ub-conjugated proteins were determined in liver samples from wild-type (WT) or *Ahr*-null mice (A). WT (B) and *Ahr*-null (C) mice were treated with TCDD (80 $\mu\text{g}/\text{kg}$) or griseofulvin (5 mg/kg) as a positive control.

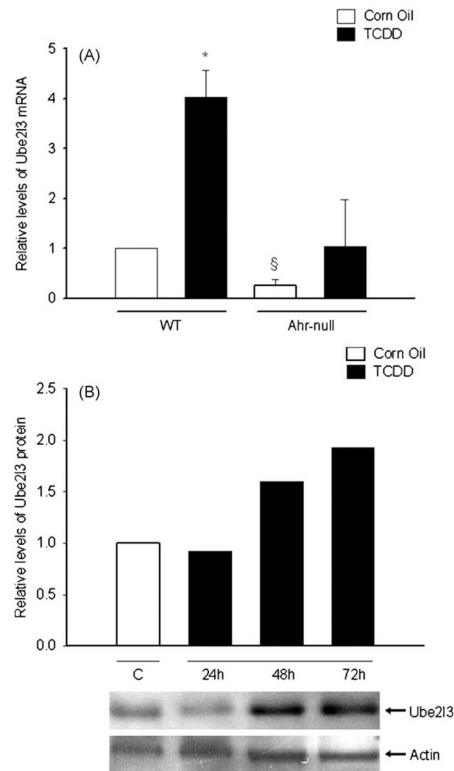


Fig. 3. TCDD affects Ube213 expression in mouse liver. Mice were treated with TCDD (80 $\mu\text{g}/\text{kg}$) or vehicle. After 24,48 or 72 h liver samples were removed and relative expression of mRNA at 24 h (A), and protein levels (B) were determined as described in Section 2. Protein and mRNA levels were normalized with actin and 18S ribosomal RNA, respectively. Data represent mean values \pm S.D. * $P < 0.05$ vs. control (vehicle), § $P < 0.05$ vs. wild-type (WT).

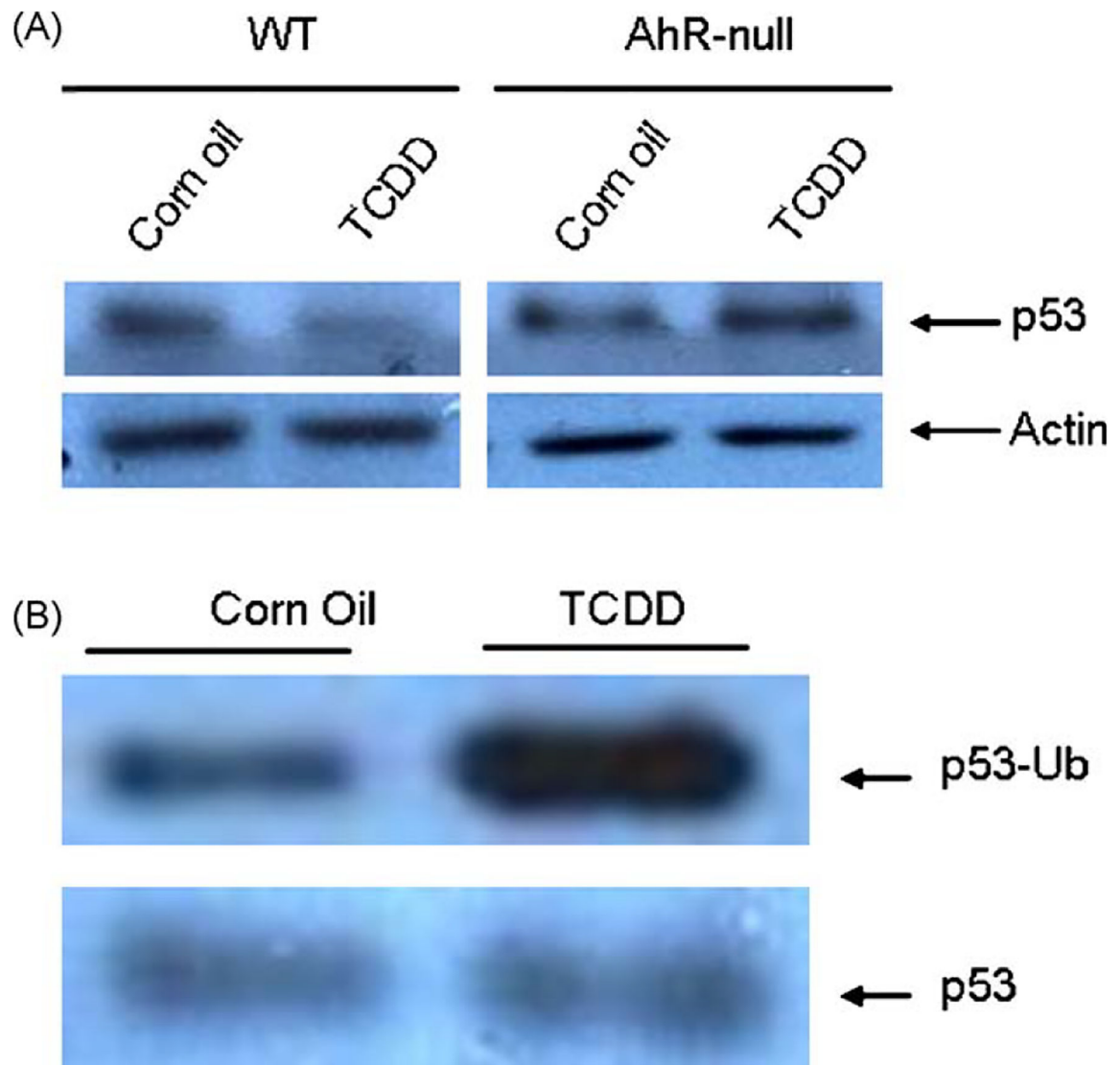


Fig. 5. TCDD affects p53 and Ub-p53 protein levels. Wild-type (WT) or *Ahr*-null mice were treated with TCDD (80 $\mu\text{g}/\text{kg}$) or vehicle. Liver samples were removed 72 h later and p53 protein (A) or Ub-p53 proteins levels (B) were determined as described in Section 2.

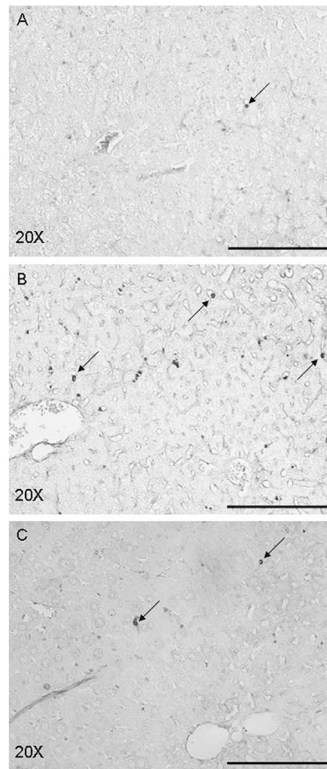


Fig. 6. Apoptosis in hepatocytes from WT mice exposed to B[a]P. Apoptotic cells were detected by the TUNEL assay as described in Section 2. Mice were pre-treated with 80 $\mu\text{g}/\text{kg}$ TCDD 3 days before sacrifice and/or 230 mg/kg B[a]P for 24 h. WT control sample (A), WT B[a]P treated sample (B), and WT TCDD + B[a]P treated sample (C).

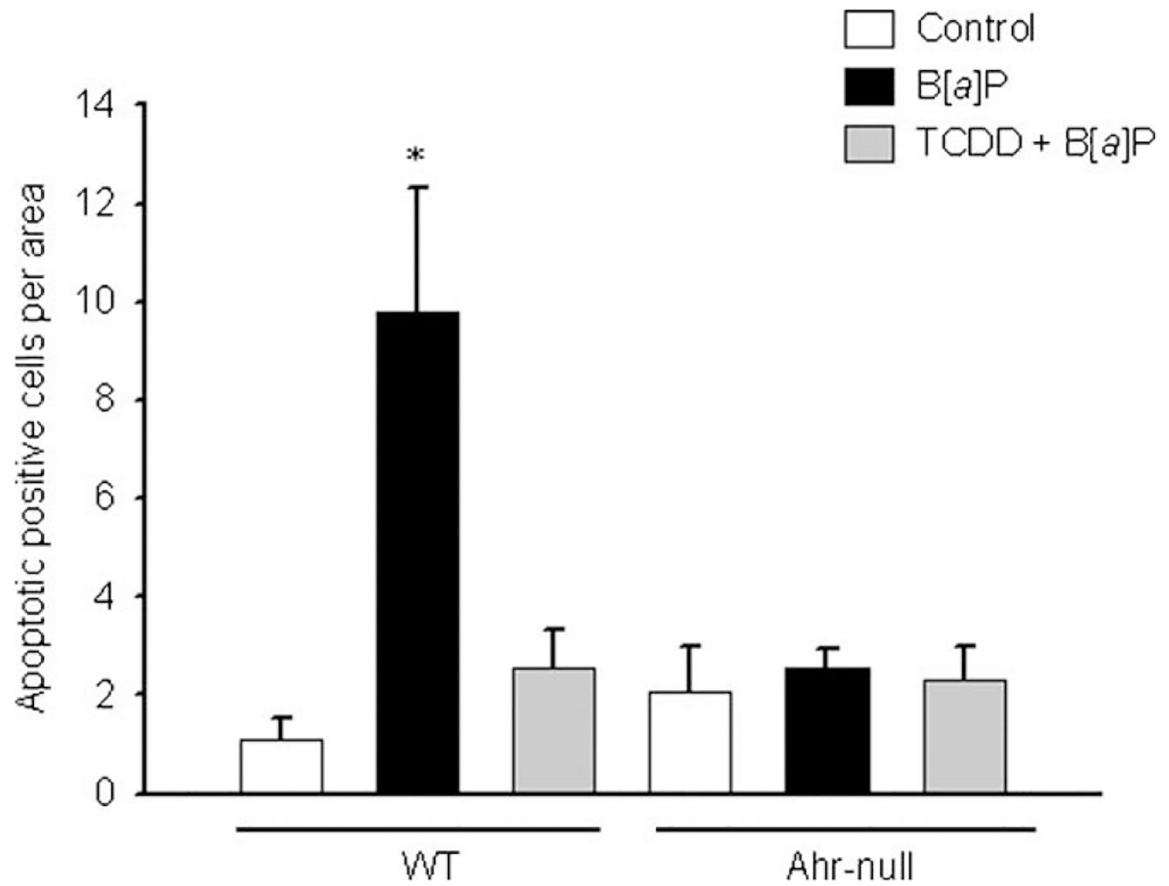


Fig. 7. Pre-treatment with TCDD decreases apoptosis in response to B[a]P. Apoptotic cells were counted in 10 different fields from wild-type (WT) and *Ahr*-null mice liver samples. Data represent mean values \pm S.E. from three different animals.

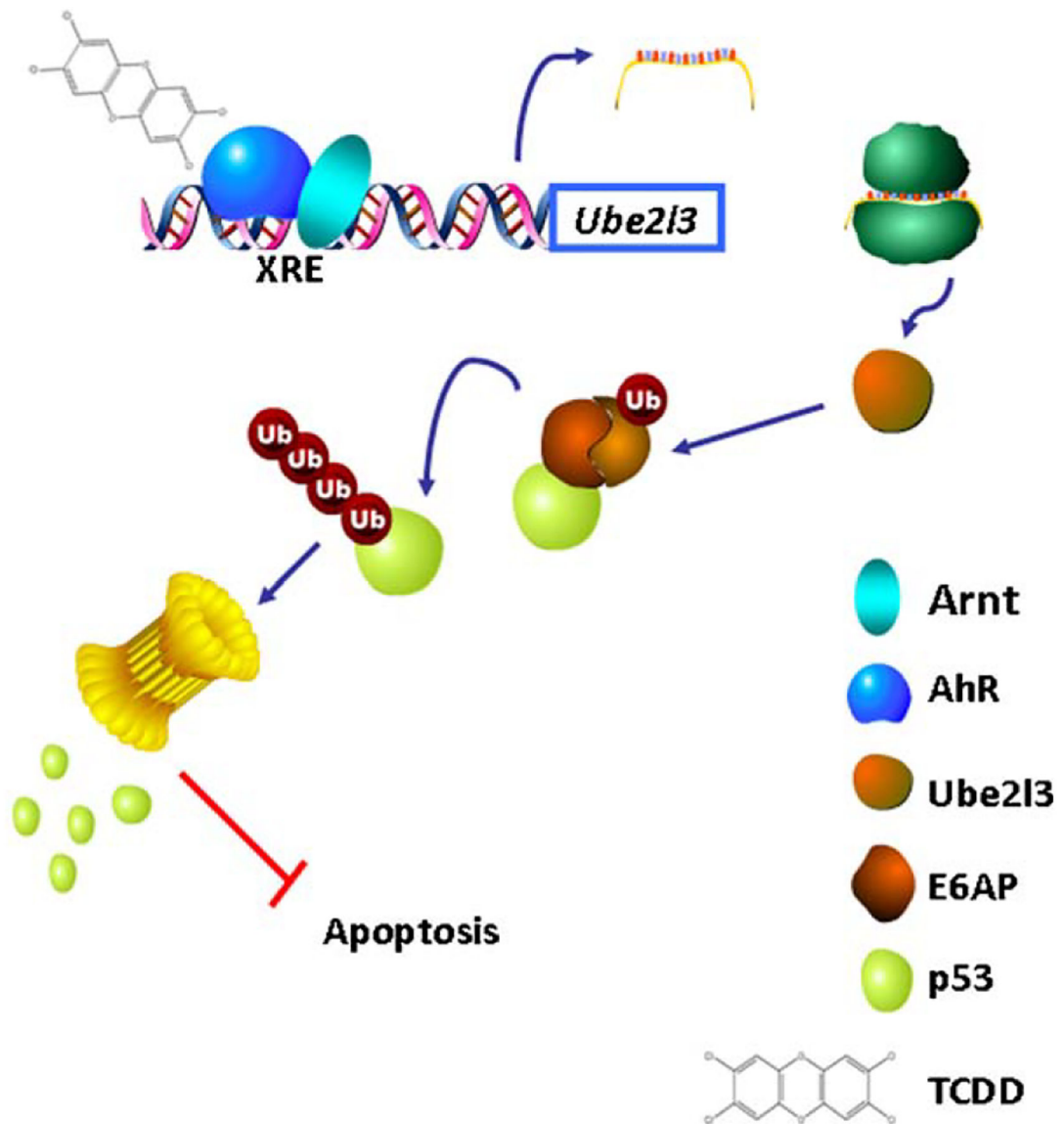


Fig. 8. Model of p53 regulation by AhR activation. Upon binding TCDD, the AhR translocates to the nucleus, dimerizes with the AhR nuclear translocator protein (ARNT), binds xenobiotic responsive elements (XREs) localized at the *Ube213* gene promoter increasing Ube213 levels. The Ube213-E6AP complex formation leads to an increase of p53 ubiquitination and degradation by the proteasome 26S resulting in apoptosis inhibition.

Table 1

Basal gene expression in the livers of AhR-KO mice as compared to the control AhR.

Accession no.	Symbol	Gene name	z-score
Ubiquitin and ubiquitin like system			
NM_009455	Ube2e1	Ubiquitin-conjugating enzyme E2E 1, UBC4/5 homolog (yeast)	-3.106235
NM_009993	Ube2l3	Ubiquitin-conjugating enzyme E2L 3	-6.65791
NM_012012	Ube3a	Ubiquitin-protein ligase E3A	-5.227039
AK018743	Pias2	Protein inhibitor of activated STAT 2	-2.709916
AK005791	SYVN1	Synovial apoptosis inhibitor 1, synoviolin	-2.131618
NM_024477	Anapc5	Anaphase-promoting complex subunit 5	-1.702395
Proteasome			
NM_026519	Psmd12	Proteasome (prosome, macropain) 26S subunit, non-ATPase, 12	-3.34548
NM_013875	Psmb3	Proteasome (prosome, macropain) subunit, beta type 3	-2.09799
NM_013873	Psmb2	Proteasome (prosome, macropain) subunit, beta type 2	-2.62315
Metabolism of xenobiotics by cytochrome P450 - Mus musculus (mouse)			
Fase I			
NM_010750	Cyp1a1	Cytochrome P450, family 1, subfamily a, polypeptide 1	-2.248441
NM_010759	Cyp1a2	Cytochrome P450, family 1, subfamily a, polypeptide 2	-1.873759
NM_023371	Cyp2e1	Cytochrome P450, family 2, subfamily e, polypeptide 1	-1.854343
FaseII			
NM_008487	Gstm2	Glutathione S-transferase, mu 2	-2.585971
NM_008510	Gstt1	Glutathione S-transferase, theta 1	-3.387056
Glycolysis/gluconeogenesis			
NM_016859	Hk2	Hexokinase 2	-1.546956
NM_021396	Pfkip	Phosphofructokinase, platelet	-1.673929
NM_020007	Pgam2	Phosphoglycerate mutase 2	-1.504628